



Broadly effective metabolic and immune recovery with C5 inhibition in CHAPLE disease

Ahmet Ozen^{1,2,3}✉, Nurhan Kasap^{1,2,3}, Ivan Vujkovic-Cvijin⁴, Richard Apps⁵, Foo Cheung⁵, Elif Karakoc-Aydiner^{1,2,3}, Bilge Akkelle⁶, Sinan Sari⁷, Engin Tutar⁶, Figen Ozcay⁸, Dilara Kocacik Uygun⁹, Ali Islek¹⁰, Gamze Akgun^{2,3,11}, Merve Selcuk¹², Oya Balci Sezer⁸, Yu Zhang^{13,14}, Günsel Kutluk¹⁵, Erdem Topal¹⁶, Ersin Sayar¹⁷, Çigdem Celikel¹⁸, Roderick H. J. Houwen¹⁹, Aysen Bingol⁹, Ismail Ogulur^{1,2,3}, Sevgi Bilgic Eltan^{2,3,11}, Andrew L. Snow²⁰, Camille Lake²⁰, Giovanna Fantoni⁵, Camille Alba²¹, Brian Sellers⁵, Samuel D. Chauvin^{14,22}, Clifton L. Dalgard²³, Olivier Harari²⁴, Yan G. Ni²⁴, Ming-Dauh Wang²⁴, Kishor Devalaraja-Narashimha²⁴, Poorani Subramanian^{14,25}, Rabia Ergelen²⁶, Reha Artan²⁷, Sukru Nail Guner²⁸, Buket Dalgic⁷, John Tsang⁵, Yasmine Belkaid^{4,5}, Deniz Ertem⁶, Safa Baris^{1,2,3} and Michael J. Lenardo^{14,22}✉

Complement hyperactivation, angiopathic thrombosis and protein-losing enteropathy (CHAPLE disease) is a lethal disease caused by genetic loss of the complement regulatory protein CD55 leading to overactivation of complement and innate immunity together with immunodeficiency due to immunoglobulin wasting in the intestine. We report in vivo human data accumulated using the complement C5 inhibitor eculizumab for the medical treatment of patients with CHAPLE disease. We observed cessation of gastrointestinal pathology together with restoration of normal immunity and metabolism. We found that patients rapidly renormalized immunoglobulin concentrations and other serum proteins as revealed by aptamer profiling, re-established a healthy gut microbiome, discontinued immunoglobulin replacement and other treatments and exhibited catch-up growth. Thus, we show that blockade of C5 by eculizumab effectively re-establishes regulation of the innate immune complement system to substantially reduce the pathophysiological manifestations of CD55 deficiency in humans.

In 1961, T. A. Waldmann¹ described serum hypoproteinemia associated with protein-losing enteropathy (PLE)¹. The disease pathogenesis was unknown, and temporizing measures such as albumin infusions and immunoglobulin replacement therapy (IgRT) became the conventional therapies. In 2017, the discovery of 'CD55 deficiency with hyperactivation of complement, angiopathic thrombosis, and PLE' (CHAPLE disease, MIM 226300) revealed that complement and innate immunity hyperactivation caused by

¹Division of Allergy and Immunology, Department of Pediatrics, School of Medicine, Marmara University, Istanbul, Turkey. ²Istanbul Jeffrey Modell Diagnostic Center for Primary Immunodeficiency Diseases, Istanbul, Turkey. ³The Isil Berat Barlan Center for Translational MHedicine, Berat, Albania. ⁴Metaorganism Immunity Section, Laboratory of Immune System Biology, National Institute of Allergy and Infectious Diseases (NIAID), National Institutes of Health (NIH), Bethesda, MD, USA. ⁵Trans-NIH Center for Human Immunology, Autoimmunity, and Inflammation, NIH, Bethesda, MD, USA. ⁶Division of Gastroenterology, Hepatology and Nutrition, Department of Pediatrics, School of Medicine, Marmara University, Istanbul, Turkey. ⁷Division of Gastroenterology, Hepatology and Nutrition, Department of Pediatrics, School of Medicine, Gazi University, Ankara, Turkey. ⁸Division of Gastroenterology, Hepatology and Nutrition, Department of Pediatrics, Baskent University Hospital, Ankara, Turkey. ⁹Division of Allergy and Immunology, Department of Pediatrics, School of Medicine, Akdeniz University, Antalya, Turkey. ¹⁰Division of Gastroenterology, Hepatology and Nutrition, Department of Pediatrics, Ataturk University, Erzurum, Turkey. ¹¹Division of Allergy and Immunology, Department of Pediatrics, Ministry of Health, Marmara University, Istanbul, Turkey. ¹²Department of Pediatrics, School of Medicine, Marmara University, Istanbul, Turkey. ¹³Human Immunological Diseases Section, Laboratory of Clinical Immunology and Microbiology, NIAID, NIH, Bethesda, MD, USA. ¹⁴Clinical Genomics Program, NIAID, NIH, Bethesda, MD, USA. ¹⁵Division of Gastroenterology, Hepatology and Nutrition, Department of Pediatrics, Kanuni Sultan Süleyman Training and Research Hospital, Health Sciences University, Istanbul, Turkey. ¹⁶Division of Allergy and Immunology, Department of Pediatrics, School of Medicine, Inonu University, Malatya, Turkey. ¹⁷Division of Gastroenterology, Hepatology and Nutrition, Department of Pediatrics, Alanya Alaaddin, Keykubat University, Alanya, Turkey. ¹⁸Department of Pathology, School of Medicine, Marmara University, Istanbul, Turkey. ¹⁹Department of Pediatric Gastroenterology, University Medical Center–Wilhelmina Children's Hospital, Utrecht, the Netherlands. ²⁰Department of Pharmacology and Molecular Therapeutics, Uniformed Services University of the Health Sciences, Bethesda, MD, USA. ²¹The American Genome Center, Henry Jackson Foundation, Uniformed Services University of Health Sciences, Bethesda, MD, USA. ²²Molecular Development of the Immune System Section and NIAID Clinical Genomics Program, Laboratory of Immune System Biology, NIAID, NIH, Bethesda, MD, USA. ²³Department of Anatomy, Physiology and Genetics, The American Genome Center, Uniformed Services University of the Health Sciences, Bethesda, MD, USA. ²⁴Regeneron Pharmaceuticals, Inc, Tarrytown, NY, USA. ²⁵Bioinformatics and Computational Biosciences Branch, Office of Cyber Infrastructure and Computational Biology, NIAID, NIH, Bethesda, MD, USA. ²⁶Department of Radiology, School of Medicine, Marmara University, Istanbul, Turkey. ²⁷Division of Pediatric Gastroenterology, Hepatology and Nutrition, Department of Pediatrics, School of Medicine, Akdeniz University, Antalya, Turkey. ²⁸Division of Pediatric Allergy and Immunology, Meram Medical Faculty, Necmettin Erbakan University, Konya, Turkey.

✉e-mail: ahmet.ozen@marmara.edu.tr; lenardo@nih.gov

CD55 (also known as decay acceleration factor) gene deficiency can cause this disorder^{2,3}. The cardinal features are severe PLE due to primary intestinal lymphangiectasia due to the inflammatory attack on intestinal lymphatic vessels by complement and innate immune overactivation^{2,4}. CHAPLE leads to severe pathophysiology, including diarrhea with protein-wasting, vomiting, abdominal pain and edema that cause a metabolic starvation state; recurrent infections due to hypogammaglobulinemia; and severe, often fatal, thromboembolic complications^{1,2,4}. The disease occurs globally but prevails in areas with high consanguinity, such as the Iğdir region of eastern Turkey, where there is a high carrier frequency of *CD55* loss of function alleles. Lethal CHAPLE disease, ‘tedirgin’ in the local language (meaning agitated), is prevalent there, and desperate parents of affected children resort to folk remedies since conventional therapies do not improve or extend life. Thus, understanding the immune and metabolic derangements due to *CD55* loss and how they change with complement interventions is critical.

The complement system is a cascade of proteins coordinated with innate and adaptive immunity to destroy pathogens and clear immune complexes, apoptotic cells and debris^{5,6}. Complement activation produces bioactive peptides—anaphylatoxins—that can alter both innate and adaptive immune responses and ultimately lead to the assembly of a membrane attack complex (MAC) that can lyse targets such as pathogens or cells⁷. Unwanted complement activation on host/self cells is regulated by the cell surface glycoproteins *CD55* (decay acceleration factor), *CD46* and *CD59*, which protect normal hematopoietic, endothelial and epithelial cells from complement-mediated damage⁸. In the gastrointestinal (GI) tract, lymph recirculation through lymph vessels called lacteals return serum proteins such as albumin and immunoglobulin to venous circulation. The genetic loss of *CD55* induces local complement hyperactivation that deposits MAC on GI lymphatics, causing PLE². Other severe diseases, such as paroxysmal nocturnal hemoglobinuria (PNH) and atypical hemolytic uremic syndrome, result from the loss of complement inhibitors and uncontrolled complement activation on erythrocytes and kidney basal membrane cells, respectively^{2,9–12}. Both conditions are treated effectively with the complement inhibitor eculizumab (Soliris). Eculizumab is a monoclonal antibody that binds to and inhibits the activation of C5, which occurs normally as consequence of the activation of the central complement component C3. *CD55* is a negative regulator of the C3 and C5 convertases that mediate cleavage activation of C3 and C5. We found that eculizumab successfully abrogated complement activation *in vitro* in T cells from patients with CHAPLE disease².

Previous studies reported that eculizumab improved the condition of three members of a family with *CD55* deficiency^{3,13}. These promising results raised several important questions. Would eculizumab have broad efficacy in families with different genetic backgrounds and *CD55* mutations? What physiological manifestations of disease would be alleviated, and would healthy immunity and metabolism be re-established. What are the drug pharmacokinetics

and pharmacodynamics for complement control? Are there pharmacogenomic variants that determine treatment efficacy and dosing? Because PLE causes a starvation state, what are the specific metabolic effects of the disease and treatment? Multiplexed proteomic platforms have identified new biomarkers and new disease mechanisms. For example, the investigation of inflammatory bowel disease using ‘slow off-rate modified aptamers’ (SOMAmers) revealed key serum protein changes independent of transcriptome changes, suggesting this could help elucidate CHAPLE disease mechanisms¹⁴. Finally, despite ubiquitous *CD55* expression in the body, the severe complement hyperactivation in CHAPLE disease affects mainly the GI tract. Could microbiome studies yield insights into GI pathogenesis^{2,15,16}? We therefore comprehensively investigated eculizumab as a medical treatment in patients with CHAPLE disease with different *CD55* gene mutations.

Results

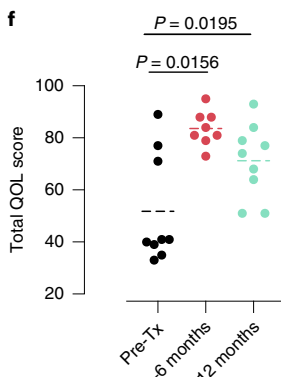
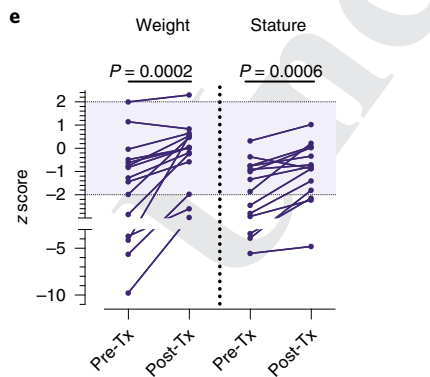
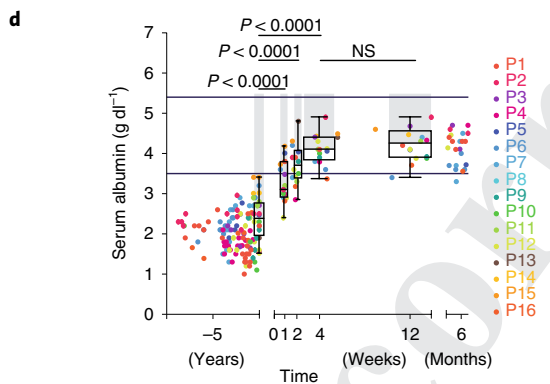
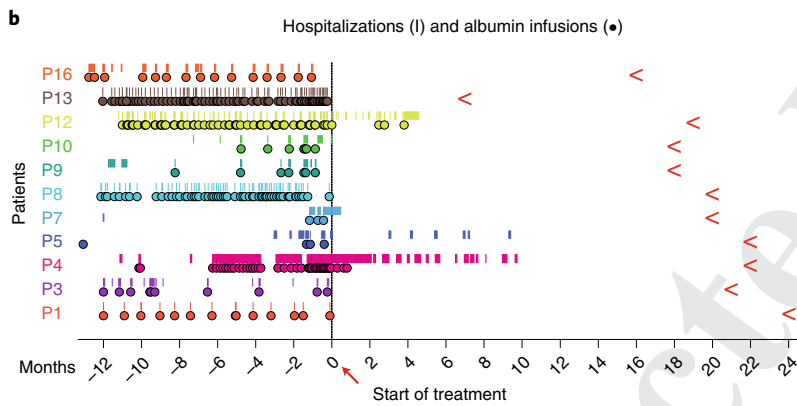
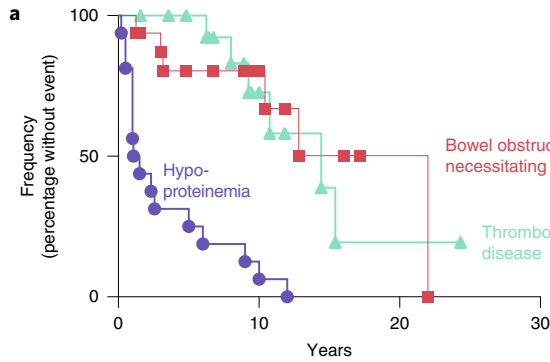
Natural history of a case series of CHAPLE disease. We evaluated 16 patients with CHAPLE disease from 14 families diagnosed with recessive biallelic *CD55* gene mutations causing decreased *CD55* expression and complement overactivation (Extended Data Fig. 1 and Supplementary Fig. 1)². All patients manifested severe PLE leading to hypoproteinemia, low immunoglobulin concentrations and recurrent infections, abdominal pain, nausea, vomiting, diarrhea, loss of appetite, weight loss and edema (Extended Data Figs. 1 and 2 and Supplementary Information)^{2,3}. Patients progressed to three life-threatening conditions: hypoproteinemia causing metabolic derangements, starvation and infections; debilitating GI inflammation, ulceration and obstruction; and severe, often fatal, thromboembolic disease (Fig. 1a, Extended Data Fig. 2 and Supplementary Information, case histories). Patients required frequent hospitalizations and many medical interventions, including albumin infusions and IgRT, that failed to alleviate disease (Fig. 1b and Extended Data Fig. 3). In the extended families, we found 32 probable patients with CHAPLE disease, of whom 8 died in childhood (25%) and many others were severely ill.

Eculizumab causes rapid improvement in most symptoms and overall health. During medical care, we filed appeals to the Turkish Medicines and Medical Devices Agency to provide eculizumab not as a clinical trial but for off-label use in the care of each of the 15 patients. The 16th patient was treated in the Netherlands using eculizumab provided by medical insurance. We observed treatment effects over a median of 20 months (interquartile range 18–22 months) totaling 309 patient–months of data. Strikingly, most patients no longer required hospitalization or transfusions of albumin or immunoglobulin following eculizumab therapy (Fig. 1b). Three patients did not receive the full regimen due to inaccessibility (patient (P) 5) or medical reasons (P12), or there was only a partial drug response (P4 and Supplementary Information); however, all three responded to treatment adjustments. Long-standing

Fig. 1 | The treatment effect of eculizumab in CHAPLE disease. **a**, A Kaplan–Meier plot showing cumulative frequency of being without hypoproteinemia (purple), bowel obstruction (red) and thromboembolic disease (green) versus time (years) ($n = 16$). **b**, Timeline of hospitalizations (vertical line) and albumin infusions (circles) for 11 patients pretreatment (pre-Tx) (–) and post-treatment (post-Tx) (+) time (months). Red leftward arrowheads indicate the end of the observation period. **c**, Heatmaps of the prevalence (percentage of patients, $n = 16$) in the study population of the indicated clinical parameter or therapeutic intervention, respectively, over patient lifetime (past), past year pre-Tx and the post-Tx observation period when a particular patient has been on regular eculizumab treatment. **d**, Serum albumin concentration before and after treatment beginning at $t = 0$. Horizontal bars show normal range; gray bars indicate statistical comparison range using mixed-effects analysis with Tukey’s multiple comparisons correction ($n = 16$). The statistical comparison of 4 versus 12 weeks revealed an adjusted P value of 0.3905 (NS, not significant). For each timepoint, the box plot shows the median, interquartile range, minimum and maximum values. **e**, Plots of weight and height (stature) z -scores compared to population averages pre-Tx and after 20 months of treatment using a paired t -test ($n = 12$). Gray region indicates the normal range. Z -scores were calculated using an online calculator (<https://pedtools.org/growthpedi/index.php>) that uses Centers for Disease Control and Prevention (CDC) data tables as chart source. **f**, Total QOL score of patients using the KINDL-R questionnaire ($n = 9$ for pre-Tx and 12 months’ assessments; $n = 8$ at 1–6 months). The statistical comparisons were made by Wilcoxon matched-pairs signed-rank test. All P values are two-sided. MCT, medium-chain triglyceride; TNF, tumor necrosis factor; TPA, tissue plasminogen activator.

130 pathophysiological signs and symptoms were eliminated by eculi-
 131 zumab (Fig. 1c and Extended Data Figs. 1 and 2). Most previous
 132 treatment interventions became unnecessary (Fig. 1c and Extended
 133 Data Fig. 3). However, supplementation of iron and vitamin D, thy-
 134 roxin, anticoagulants and thrombolytic medications continued to

be needed by some patients. Within months, the children exhibited
 a healthier appearance and function. Serum albumin increased into
 the normal range within 2–4 weeks, and remained normal at least
 6 months or longer (Fig. 1e and Extended Data Fig. 1). The patients’
 heights and weights improved, and the total quality of life (QOL)



c

| Clinical feature | Past | Past year, Pre-Tx | Post-Tx |
|---------------------|------|-------------------|---------|
| Abdominal pain | 100 | 100 | 0 |
| Nausea | 88 | 88 | 0 |
| Vomiting | 88 | 88 | 0 |
| Diarrhea | 88 | 86 | 0 |
| Loss of appetite | 75 | 75 | 0 |
| Edema | 88 | 88 | 0 |
| Albumin transfusion | 94 | 69 | 6 |
| Thromboembolism | 38 | 38 | 25 |
| Thrombocytosis | 80 | 88 | 6 |
| Bowel obstruction | 38 | 50 | 0 |
| Low albumin | 100 | 100 | 0 |
| Low total protein | 100 | 100 | 0 |
| Low IgG | 100 | 100 | 6 |
| Low vitamin B12 | 80 | 73 | 0 |

Intervention

| | | | |
|-------------------------------|----|----|----|
| Bowel resection surgery | 33 | 6 | 0 |
| Other invasive interventions | 20 | 13 | 0 |
| Multivitamins | 67 | 50 | 0 |
| Vitamin D | 93 | 81 | 25 |
| Vitamin B12 | 80 | 50 | 6 |
| Folate | 27 | 13 | 0 |
| Iron | 87 | 69 | 25 |
| Calcium, magnesium, zinc | 67 | 50 | 0 |
| Omega-3 fatty acid | 27 | 13 | 0 |
| MCT oil | 33 | 38 | 0 |
| Enteral formula feeding | 60 | 44 | 0 |
| Parenteral nutrition | 27 | 19 | 0 |
| Erythrocyte transfusion | 27 | 6 | 0 |
| Albumin transfusion | 93 | 69 | 0 |
| Immunoglobulin Rx | 60 | 56 | 0 |
| Corticosteroids | 87 | 63 | 0 |
| Mesalazine | 60 | 31 | 0 |
| Azathioprine | 47 | 19 | 0 |
| Methotrexate | 13 | 13 | 0 |
| Anti-TNF | 33 | 19 | 0 |
| Low-molecular weight heparin | 14 | 25 | 19 |
| Low-dose acetylsalicylic acid | 20 | 31 | 13 |
| TPA lysis of clots | 7 | 6 | 6 |
| Respiratory support | 13 | 6 | 6 |
| Octreotide to alleviate PLE | 33 | 25 | 0 |
| Antibiotic prophylaxis | 53 | 31 | 0 |
| Tx for unusual infections | 53 | 38 | 0 |
| Thyroxin for hypothyroidism | 27 | 13 | 13 |

135 scores increased (Fig. 1f,g, Extended Data Fig. 2 and Supplementary
136 Figs. 2 and 3). However, thrombocytosis, thrombosis and pulmo-
137 nary embolism persisted in some patients (Fig. 1c and Extended
138 Data Fig. 2). Overall, eculizumab treatment substantially restored
139 normal physiology and immunity.

140 CHAPLE disease involves complement damage to GI lymphat-
141 ics, so we evaluated the intestinal mucosa by endoscopy². We found
142 that lymphangiectasia, reflected by the dense white aggregates
143 imparting a grayish cast on the mucosa, was eliminated by treat-
144 ment (Fig. 2a). Eculizumab also promoted the healing of muco-
145 sal ulcers (Supplementary Fig. 4). Prospective symptom diaries
146 revealed that the treatment reduced all GI symptoms and edema
147 within 4 weeks (Fig. 2b, Extended Data Fig. 2 and Supplementary
148 Fig. 5). Restoration of normal alimentary function was illustrated by
149 increases in vitamin B12 and serum immunoglobulin, making IgRT
150 and vitamin supplements unnecessary (Fig. 2c,d and Extended
151 Data Fig. 1). We found markedly improved immune function, with
152 reduced and less severe infections. Patients with CHAPLE disease
153 also have abnormal increases in triglycerides and platelets that were
154 reversed by eculizumab (Fig. 2e,f). Moreover, a blood cell aggre-
155 gation abnormality was also eliminated by treatment (Fig. 2g).
156 Radiological abnormalities, including bowel wall thickening, con-
157 trast enhancement, intestinal stricture and proximal dilatation, free
158 fluid collection and abscess formation, also resolved with treatment
159 (Fig. 2h). However, eculizumab therapy did not correct thrombo-
160 embolic disease in P4, P7 and P14, or ischemic gliotic foci in P12.
161 Thus, eculizumab effectively ameliorated most disease findings
162 except for thromboembolic disease.

164 Dosing intervals, interrupted therapy and pharmacokinetics.

165 We next studied the pharmacokinetics and pharmacodynamics of
166 eculizumab and total C5 (free + eculizumab bound). In a previ-
167 ous report, Kurolap et al. used an augmented induction regimen
168 to account for GI protein-wasting with twice-weekly injections¹³.
169 However, we found that once-weekly induction doses achieved a
170 median trough concentration of eculizumab of 217 and 330 $\mu\text{g ml}^{-1}$,
171 at week 1 and weeks 2–4, respectively, which were much greater than
172 100 $\mu\text{g ml}^{-1}$, the minimum recommended concentration (Fig. 3a).
173 Eculizumab complexed with C5 to increase the total C5 (free + ecu-
174 lizumab bound) in the blood to a median of 219 $\mu\text{g ml}^{-1}$ (Fig. 3b).
175 Even with the first dose, the eculizumab and total C5 concentra-
176 tions reached $\sim 200 \mu\text{g ml}^{-1}$ and were stable with the maintenance
177 doses (Fig. 3a,b). We also observed that if dosing was delayed, ecu-
178 lizumab and total C5 concentrations fell slowly and reached base-
179 line at 35 days (Fig. 3a,b). Total C5 for all patients reached a plateau
180 when eculizumab reached 60–100 $\mu\text{g ml}^{-1}$ and the ratio of total C5
181 to eculizumab dropped below 2:1 (the theoretical ratio at which
182 C5 becomes saturated by eculizumab) at 100 $\mu\text{g ml}^{-1}$ eculizumab
183 (Fig. 3c and Supplementary Fig. 6a). We therefore tested the activity

of the classic complement pathway, employing the total hemolytic
complement (CH50) test, and found it was completely inhibited by
eculizumab $> 100 \mu\text{g ml}^{-1}$ (Fig. 3d). Both the AH50 and CH50, mea-
suring the target lysis-inducing activity of the alternative and classical
pathways, respectively, were correlated with eculizumab concentra-
tions and strongly suppressed at 1 week (Fig. 3e and Supplementary
Fig. 6b,c). If dosing was delayed, eculizumab and total C5 concentra-
tions progressively decreased, and AH50 and CH50 test value out-
comes progressively increased with time (Fig. 3f and Extended Data
Fig. 4). Thus, eculizumab rapidly and potentially inhibits uncontrolled
complement activation and reverses PLE *in vivo*.

We also tried extended dosing intervals^{11,12}. Using 4-week dos-
ing, we found no disease relapse in P1, P3, P5, P8, P9, P10 and P11
(Extended Data Figs. 4 and 5a). By contrast, P4, the most severely
affected in our cohort, showed disease relapse unless we used a
10-day dosing interval (Extended Data Fig. 5b). This finding was
not explained by the *CD55* mutation in P4, since the identical amino
acid change is present in P2 and P5, who responded normally to ecu-
lizumab (Extended Data Fig. 1). In P4, we observed less CH50 and
AH50 inhibition at comparable concentrations of serum eculizumab
than in other patients (Fig. 3d,e). Also, total C5 accumulation was
much higher in P4, suggesting eculizumab bound to C5 (Fig. 3b,c).
We, therefore, performed whole-genome sequencing (WGS) on P4
and his affected sister, P5, who had responded better to treatment.
We detected no new or extremely rare variants but a single-nucleotide
polymorphism (SNP) (rs17611) encoding a V802I amino acid substi-
tution in C5 that was homozygous in P4 and heterozygous in P5. This
SNP is common (minor allele frequency = 0.4590 in the gnomAD
database) with global homozygosity of about 23% (32,516 homo-
zygous in 141,333 total individuals, https://gnomad.broadinstitute.org/variant/9-123769200-C-T?dataset=gnomad_r2_1) and previ-
ously associated with inflammatory diseases, including liver fibrosis
and rheumatoid arthritis^{17,18}. The substituted residue is outside of
the eculizumab binding site but alters the structure so that five new
amino acid clashes occur in the complex (Supplementary Fig. 7a–c)¹⁹.
Further genotyping showed that P8, P13 and P14 were also homozy-
gous for I802 (Supplementary Fig. 7d). These patients had compara-
tively higher antibody–C5 complex concentrations, reduced C5a and
slightly higher soluble C5b–9 complex (sC5b–9) but did not require
increased administration of eculizumab (Supplementary Fig. 7e–g).
Previous *in vitro* work showed that eculizumab blocks C5₈₀₂ activity,
but the variant protein is cleaved less efficiently by human neutrophil
elastase^{17,20}. Taken together, the C5_{802I/802I} variant appears to alter
the antibody–C5 complex and possibly its turnover²¹; however, more
complicated factors are likely involved in the poor response of P4 to
eculizumab therapy.

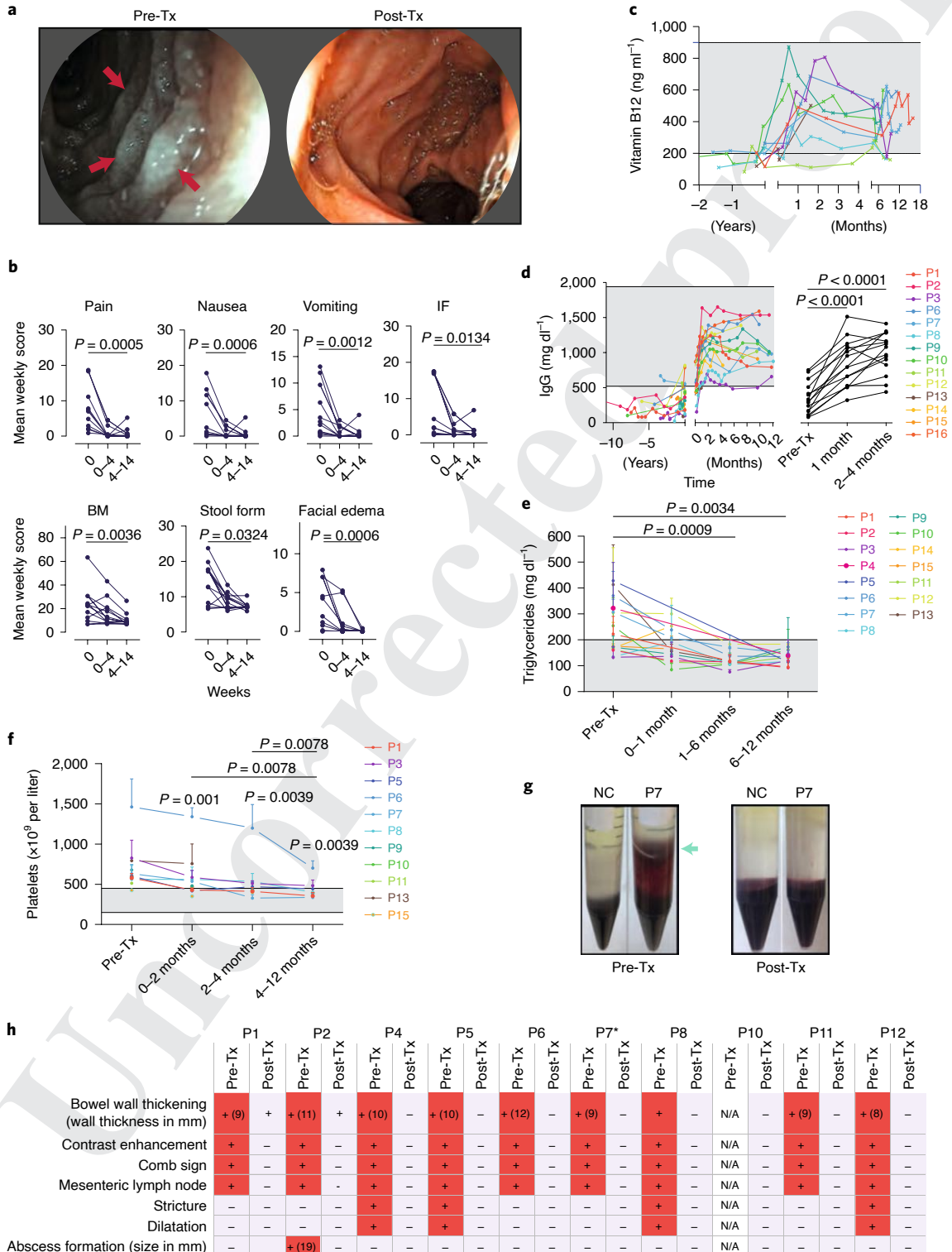
Eculizumab therapy was interrupted due to medication inacces-
sibility (P3 and P8) or a medical decision because of myocarditis
(P12), and all experienced disease relapse (Extended Data Fig. 5c,

186 **Fig. 2 | GI, circulatory, hematologic and metabolic manifestations of CHAPLE disease with or without eculizumab.** **a**, Duodenal endoscopy images pre-Tx
187 showing white lymph globules due to lymphangiectasia (red arrows) and lymph leakage imparting a grayish color to the mucosa and after 14 months of
188 treatment showing lymphangiectasia replaced by normal mucosa. **b**, Mean total weekly scores as defined in the Methods for the indicated parameters in
189 each patient during the pre-Tx (○), 0–4 weeks and 4–14 weeks post-Tx are plotted. Statistics used the Friedman test and Dunn's multiple comparisons test
190 (two-sided *P* value; *n* = 13 patients at each timepoint). IF, inability to feed; BM, number of bowel movements. **c**, Vitamin B12 concentration in serum before
191 and after treatment beginning at *t* = 0 (*n* = 9). **d**, Serum IgG concentration before and after treatment beginning at *t* = 0 (*n* = 15 for pre-Tx and 2–4 month
192 assessments; *n* = 13 for 1 month assessment). **e**, Calculated mean and standard deviation for intrapatient repeated measurements of fasting blood
193 triglyceride concentrations during pre-Tx periods or the indicated number of months post-Tx for each patient (*n* = 15). In **d** and **e** statistical comparisons
194 were made by mixed-effects analysis and Dunnett's multiple comparisons test (two-sided *P* value). **f**, Mean and s.d. values for multiple platelet count
195 measurements obtained in each patient during the pre-Tx period or the indicated number of months post-Tx. Two-sided *P* values are calculated from
196 Wilcoxon matched-pairs signed-rank test, based on the calculated means of multiple measurements for a given interval (*n* = 11 patients). **g**, Photographs of
197 representative pre-Tx samples from P7 or normal control (NC) showing erythrocytes abnormally infiltrating the supernatant (arrow) during Ficoll gradient
198 separation of PBMCs and disappearance of this phenotype post-Tx. **h**, Summary of radiological features before and after treatment. Red (+) shows
199 presence of the sign and light blue (–) indicates absence. N/A, radiological studies not available. The asterisk in P7 indicates the presence of voluminous
200 abdominal fluid before therapy that resolved following treatment (not shown). Shaded areas in **c–f** show normal range.

Supplementary Fig. 8 and Supplementary Information). Thus, ongoing eculizumab therapy is necessary to sustain remission. Hence, CHAPLE disease differs from previous diseases in which the treatment can be tapered and discontinued²².

Complement markers before and during eculizumab treatment. Because complement variations contribute to disease variability, we assessed blood concentrations of C3, C4 and C5,

and their activation products together with copy number variations (CNV) in the *C4* gene (Fig. 4a–j)²³. We observed C3a, C4b, C5a and soluble terminal complex (sC5b–9) were increased and complement Factor H (CFH) was decreased in baseline disease compared to age-matched healthy controls (AMCs) (Fig. 4 and Supplementary Fig. 7f,g). After treatment, free C5, C5a, sC5b–6 and sC5b–9 were swiftly reduced. Also, we found increased C4b and CFH but no reduction in C3a with therapy (Fig. 4b,e,f,g,k).



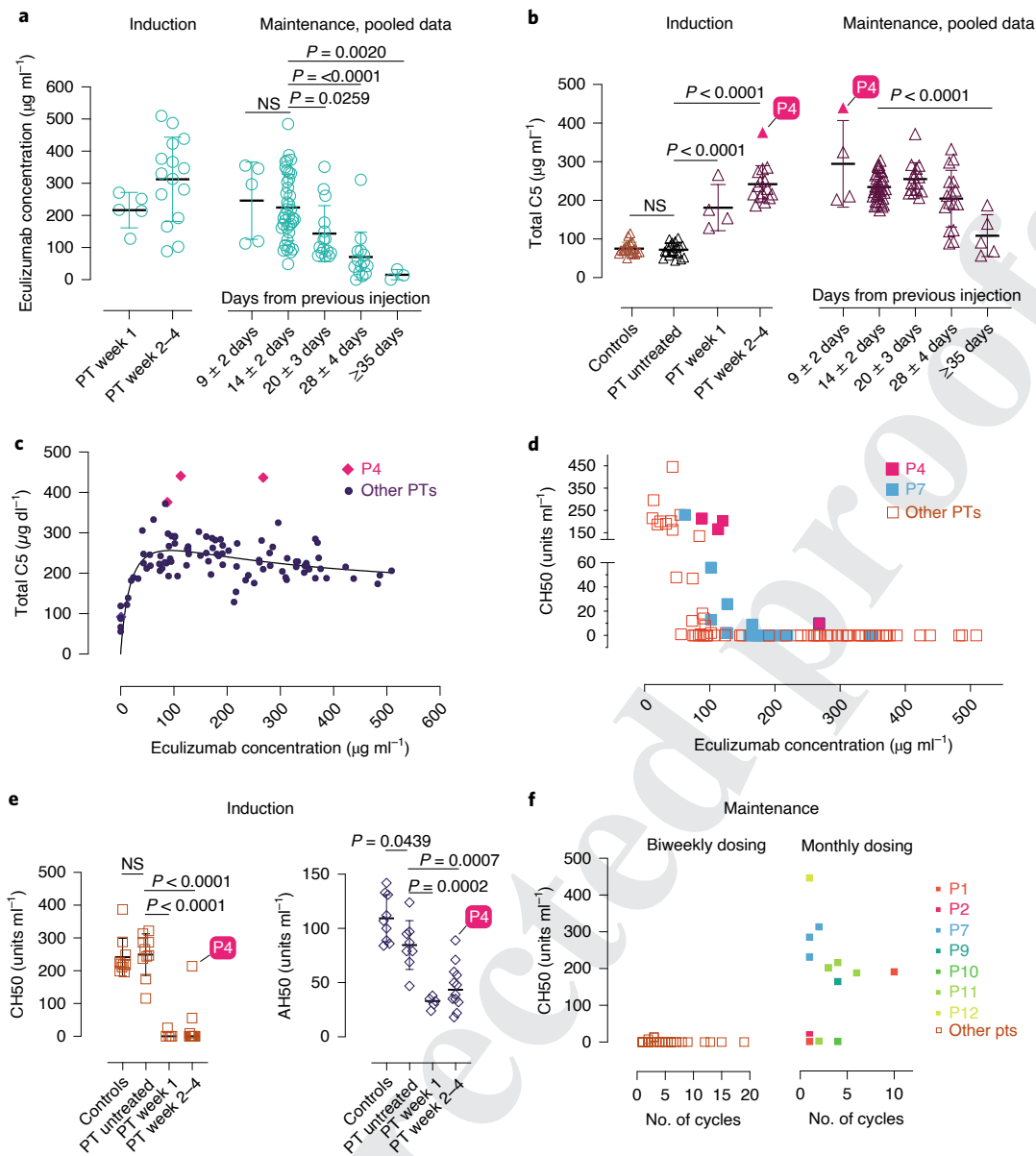


Fig. 3 | Serum ecuzimab concentration and total C5 and functional complement inhibition during the induction and maintenance phases of treatment. **a, b**, Ecuzimab and total C5 concentrations with respect to timing of therapy during the periods indicated. The respective exact P values comparing 9 \pm 2 versus 14 \pm 2 days was 0.9803 in **a**, and controls versus untreated patients was 0.9926 in **b**. **c, d**, Pooled analyses of patient samples showing total C5 (**c**) and CH50 (**d**) levels across the range of ecuzimab concentrations. **e**, CH50 and AH50 levels with respect to timing of therapy during the periods indicated. **f**, CH50 values with respect to number of cycles on the standard biweekly dosing intervals or the modified monthly dosing regimen in selected cases. Error bars indicate mean and s.d. values. Multiple group comparisons were made by ordinary one-way ANOVA test. During post hoc analyses, Dunnett's multiple comparisons test analyzed differences between the standard 14 \pm 2 days group with others in the maintenance pooled analyses in **a** and **b**, and patient (PT) untreated values with other groups in **b** and **e**, during the induction period, respectively. Adjusted P values for multiple testing are indicated. The P value comparing the controls versus untreated patients was 0.9795 in **e**. Number of samples investigated for each parameter: total C5, 19 healthy controls and 114 samples from 15 patients with CHAPLE disease; ecuzimab concentrations, 96 samples from 15 patients; CH50, 14 healthy controls and 121 samples from 15 patients; AH50, 9 healthy controls and 25 samples from 13 patients. ECmb, ecuzimab.

Intriguingly, we detected a temporary increase in total C3 and inactive C3b, but not C3b, with treatment (Fig. 4c). Perhaps the active C3b is rapidly inactivated by the inhibitory proteins, including CFH and Factor I. These changes may be secondary to dissociation of the C5-convertase complexes (by regulators other than CD55) upon abrupt removal of their substrate, the C5 molecule, from circulation since the ecuzimab-bound form is inaccessible to the enzyme. Overall, ecuzimab blocked the generation of

the terminal complement activation mediators in patients with CHAPLE disease and caused secondary upstream effects.

C4 concentrations remained stable during treatment, but four subjects, P4, P5 and P7, with a history of thrombosis, and P6 with thrombocytosis, showed increased C4 (Fig. 4c). We evaluated C4 CNV and found two patients had two C4 copies, six with three C4 copies, one with four C4 copies and one with six C4 copies determined by estimation by WGS coverage (Supplementary Fig. 7h).

The most common copy number of C4 genes, present between 50% and 60% of healthy human subjects, was four copies, but most of our patients had fewer C4 copies^{24,25}. Interestingly, consistently high serum C4 values were found in P5 and P6, even after 6 months of treatment, and they had the highest C4 copy number among all patients we followed. High serum C3 and C4 are associated with venous thrombosis in postnatal women or in the context of individuals with antiphospholipid antibodies, suggesting that the correlation of thrombosis and high C4 concentrations due to CNV in our patients could be significant^{26,27}. Our findings suggest that genetic variations in complement genes may account for disease expressivity or variable treatment responsiveness among different CD55-deficient individuals.

Mutant soluble CD55 does not prevent complement hyperactivation. The mutation in P12 inserted a stop codon for residue Gly348, which prevented addition of the glycerol phosphate-inositol membrane anchor and allowed CD55 to escape as a soluble serum form (Supplementary Fig. 9). Although typically membrane bound, CD55 is also secreted as a soluble form that inhibits complement in the fluid phase²⁸. P12 was as sick as the other patients, suggesting that this mutant soluble version of CD55 was not protective in the context of GI disease.

Microbiome changes following therapy. Pathological alterations of the gut microbiota have been observed in inflammatory and metabolic diseases¹⁵. Specifically, reductions in alpha diversity and increases in abundance of *Enterobacteriaceae* taxa occur in chronic inflammatory conditions including inflammatory bowel disease, progressive human immunodeficiency virus infection and necrotizing enterocolitis^{29–33}. We therefore performed metagenomic profiling of feces from six patients with CHAPLE disease before and after eculizumab. We observed a trend toward increased alpha diversity over 12 months of treatment ($P=0.09$, linear mixed-effects models, Fig. 5a). Pre- and post-treatment bacterial microbiota profiles clustered separately, and baseline microbiota profiles exhibited greater within-group dissimilarity (Fig. 5b,c). A similar profile was evident for fungi but not DNA viruses (Supplementary Fig. 10). Thus, eculizumab treatment causes microbiome restructuring toward a common gut microbial community, possibly by eliminating microbiome stressors, including inflammation, abnormal bowel movements, abnormal food intake and/or medications, including antibiotics. Moreover, the treatment decreased *Enterobacteriaceae* ($P=0.013$, Q value (a P value that has been adjusted for the false discovery rate (FDR))= 0.099 , Fig. 5d)—pro-inflammatory gut pathogens associated with chronic inflammatory diseases³⁴. Also, the treatment increased *Bifidobacteriaceae* ($P=0.012$, $Q=0.096$) and *Faecalibacterium prausnitzii* ($P=0.019$, $Q=0.08$), which are important microbiota in healthy infants and are depleted in

children with Crohn's disease (Fig. 5e,f)^{16,35}. Thus, eculizumab treatment shifted the microbiota composition from an inflammatory profile to an enrichment of taxa comprising a healthy microbiome³⁵.

Metabolic response to therapy. To explore metabolic abnormalities, we profiled 1305 serum proteins in eight patients using the SOMAlogic aptamer platform; 94 proteins differed significantly between patients and AMCs at baseline with $Q<0.05$ (Fig. 6a and Supplementary Fig. 11). Interestingly, despite PLE, only 26 proteins were reduced (Fig. 6a), whereas 68 proteins were increased (Fig. 6a). Of the 68 upregulated proteins, the greatest increases were in insulin-like growth factor (IGF) binding protein 2 (IGFBP2), REG4, ADSL, NACA, APOE, MMP3, PYY, GSK3A and GSK3B, CCL28 and PAPP. Of the 26 downregulated proteins, those with the greatest decreases were CA6, ADGRE2, BMP1, RET, CNTN4, APOM, NTRK3, EGFR, A2M and NTRK2, but CD55 was the lowest of any serum protein (Supplementary Fig. 12a,b). After eculizumab, the baseline patient values shifted closer to AMCs, especially for downregulated proteins (Supplementary Fig. 12c). At days 48–59, 23 of 26 downregulated proteins recovered (Fig. 6b and Supplementary Fig. 12d), but only 18 upregulated proteins were reduced (Fig. 6b and Supplementary Fig. 12d). In an unsupervised principal component analysis (PCA), patient samples at baseline (olive) moved progressively closer towards the controls (red) at 8–15 days (purple), 16–30 days (bright green) and, even more so, at 48–59 days (blue) (Fig. 6c). The PCA confirms that decreased proteins recover almost completely, whereas the increased proteins reversed but never to normal (Fig. 6c). To validate the SOMAlogic protein changes, we used an enzyme-linked immunosorbent assay (ELISA) to check IGFBP2, which had the greatest elevation in disease and responded to therapy. The ELISA confirmed elevated IGFBP2 and its correction after treatment (Fig. 6d). Moreover, in P7 and P8, we found that a treatment delay caused an abrupt increase in IGFBP2, suggesting that it is a sensitive biomarker of disease activity.

We also observed that certain proteins normal at baseline in patients with CHAPLE disease changed after eculizumab therapy. In a rank analysis, soluble erythropoietin receptor (EPOR)—a protein involved in endothelial repair—showed the greatest increase (Fig. 6e,f)^{36,37}. Among proteomic alterations, complement and coagulation pathways were the top-ranking functional groups, despite an $FDR>0.05$ (Extended Data Fig. 6a). CD55 regulates complement, innate immunity and coagulation, so we selected 53 complement and coagulation proteins measured by SOMAlogic and determined that half (24/53) showed changes at baseline or following therapy (Supplementary Fig. 13).

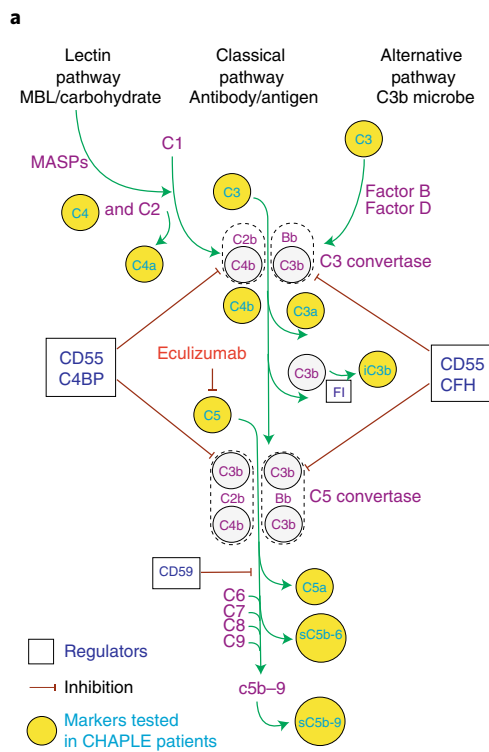
We also found substantial increases in proteins containing Ig-like domains (Supplementary Fig. 14). A tiny cluster (64 proteins) of such proteins were decreased (Extended Data Fig. 6b, blue lines). This cluster included several important immunoregulatory proteins,

Fig. 4 | Blood concentrations of complement proteins and their activated products before and during eculizumab treatment. **a**, Pathway schematic of the complement system. iC3b, inactivated C3b; FI, complement factor I; CFH, Complement factor H; MASP, mannose-associated serine protease. **b**, Summary of alterations in selected circulating complement markers in patients with CHAPLE disease. Arrows indicate the direction of change, if any: down arrow (decrease), up arrow (increase), or horizontal arrow (no change). N, normal. **c**, Blood concentration (g l^{-1}) of intact C3 and C4, at baseline and during eculizumab treatment. Mean of repeated measurements at each time interval was plotted for individual patients. A mixed-effects model assessed the significance between values at different timepoints, with Tukey's multiple comparisons test calculating adjusted P values for each pair ($n=15$ patients). **d**, Serum C4 levels in relation to estimated Complement C4 gene copy numbers based on C4 WGS coverage. In **c** and **d**, horizontal dashed lines show reference ranges. **e, j**, Blood concentration of complement products generated during complement activation at baseline and after eculizumab treatment. **k**, Soluble phase inhibitor CFH levels at baseline and during treatment. Statistics used to compare C3a between the three groups included an ordinary one-way ANOVA and the Tukey's multiple comparisons test. Adjusted P values are indicated. Mann-Whitney (for comparing AMC versus patient baseline values), and Wilcoxon matched-pairs signed-rank tests (between patient baseline versus different post-treatment timepoints) analyzed the differences between groups in **f–k** ($n=8$ control subjects and $n=8$ patients for each analysis). Red dashed symbols filled with blue in **h–j** indicate values that correspond to dropped eculizumab concentrations after dose skipping. All P values are two-sided. Sample size for C3a: 16 AMC, 21 untreated patients and 13 treated patients. Error bars indicate mean and s.d. MBL, mannose-binding lectin; RFU, relative fluorescence units.

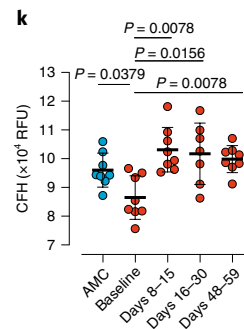
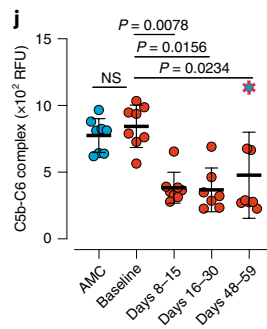
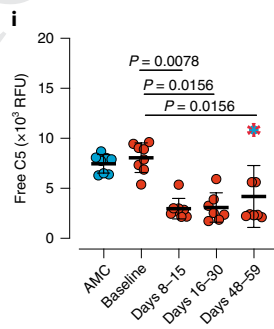
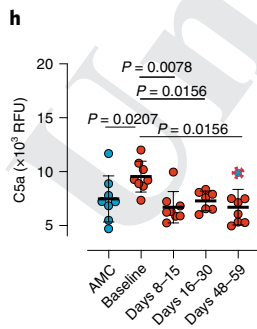
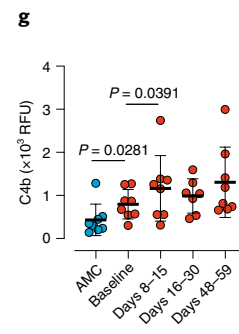
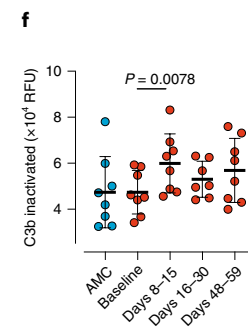
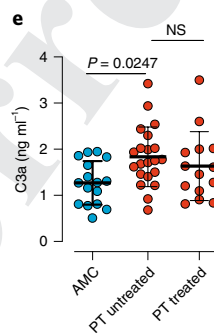
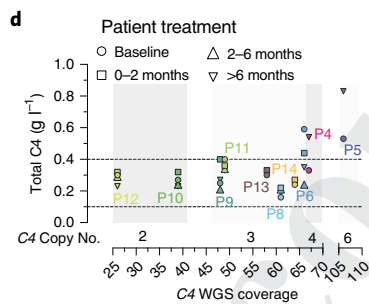
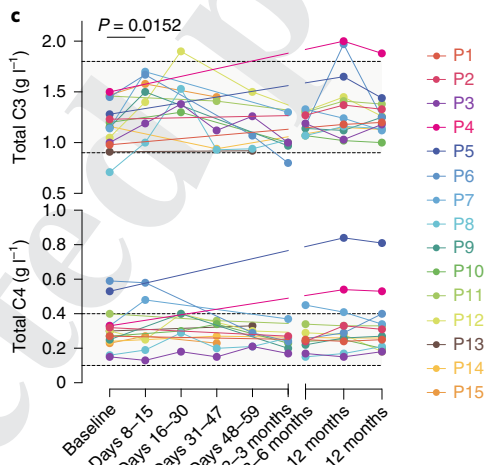
399 especially cell adhesion molecules, and showed an impressive recovery
 400 with treatment (Extended Data Fig. 6b and Supplementary
 401 Fig. 15). Interestingly, 12 of the 27 immune-related molecules altered
 402 at baseline responded to eculizumab (Supplementary Fig. 16). Thus,
 403 inhibiting complement at the C5 level corrects many, but not all,
 404 immune and inflammatory abnormalities.

Discussion

We studied the compassionate use of eculizumab ‘off label’ to treat
 16 CHAPLE cases with distinct *CD55* gene mutations. We were
 interested to understand how pharmacological inhibition down-
 stream of C5 will affect immune dysregulatory disease caused by
 CD55 loss by affecting upstream control at the C3 convertase.



| | Pretreatment | Post-Tx change from patient baseline | |
|------------------------------------|--------------|--------------------------------------|-----------|
| | | ≤ 30 days | > 30 days |
| Total C3 | N, ↓ | ↑ | → |
| C3a | ↑ | → | → |
| C3b inactivated | N | ↑ | → |
| Total C4 | N, ↑ | → | → |
| C4a | N | → | → |
| C4b | ↑ | ↑ | → |
| Total C5 (free + eculizumab bound) | N | ↑ | ↑ |
| Free C5 | N | ↓ | ↓ |
| C5a | ↑ | ↓ | ↓ |
| sC5b-6 complex | N | ↓ | ↓ |



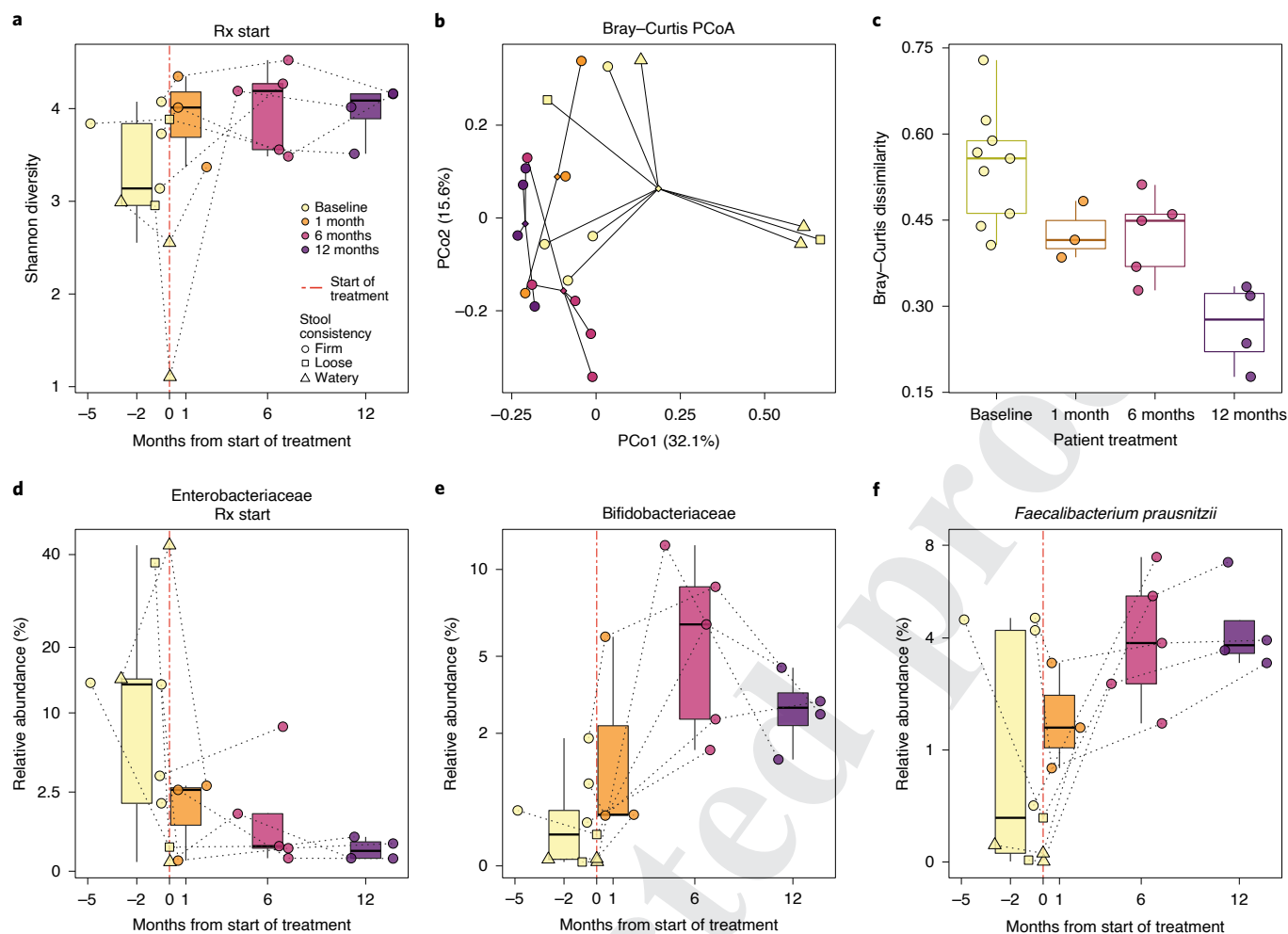


Fig. 5 | Microbiota composition shifts in ecizumab-treated patients with CHAPLE disease. **a**, Shannon alpha diversity increases pre- and post-ecizumab treatment are shown. Longitudinal samples from the same patient are connected by dotted lines. A statistical trend toward increased Shannon diversity is seen post-ecizumab treatment (linear mixed-effects (LME) unadjusted $P=0.09$). **b**, Principal coordinates analysis (PCoA) based on Bray-Curtis beta diversity metric of bacterial taxonomic abundances showing clustering by pre- and post-treatment timepoints (PERMANOVA $P=0.03$). Centroids of community distances for each timepoint group are shown as diamonds. **c**, Bray-Curtis dispersions (scaled distance from centroid) within each timepoint group (analysis of variance (ANOVA) $P=0.00066$). **d**, Enterobacteriaceae (LME $P=0.013$, FDR $Q=0.099$). **e**, Bifidobacteriaceae family abundances (LME $P=0.012$, $Q=0.096$). **f**, *Faecalibacterium prausnitzii* species abundances (LME $P=0.019$, $Q=0.08$) across time in patients with CHAPLE disease. In **a** and **c-f**, the center bar denotes the median, the boxes denote interquartile range and the whiskers denote the interquartile range $\times 1.5$. The mean of multiple assessments is used for analysis if there are more than one measurement for an individual during a particular time period. $n=6$ patients for all analyses. Q value is a P value that has been adjusted for the FDR. PCo1, principal coordinate 1; PCo2, principal coordinate 2.

465

466 Previously, three members of a single family with CHAPLE disease
 467 improved with ecizumab treatment^{3,13}. This success, and
 468 the global emergence of more CHAPLE cases, posed key immuno-
 469 logical and metabolic questions that we have now investigated. We
 470 demonstrate that ecizumab is broadly effective in patients with
 471 CHAPLE disease with different *CD55* gene mutations. Recovery
 472 from complement damage to gut lymphatics was achieved rapidly
 473 in 100% of cases. The loss of immunoglobulins, infections and
 474 long-standing functional GI abnormalities were substantially
 475 reversed, indicating that complement-mediated GI inflammation
 476 and lymphatic damage is reversible. However, the effects of the
 477 drug were temporary. We saw an immediate flare-up of symptoms
 478 and serum albumin and immunoglobulin loss when the medica-
 479 tion was withdrawn. This observation implies that complement
 480 and its innate immune and inflammatory effector mechanisms are
 481 constantly stimulated, and that patients will require continuous
 482 treatment. Thus, ecizumab effectively treats, but does not cure,

CHAPLE disease. Nonetheless, despite the high cost of ecizumab,
 our data support its early and continued use in CHAPLE disease.
 In addition, the therapeutic potential of an upstream blockade at
 the C3 level or combinatorial approaches with C3 and C5 block-
 ade at different checkpoints could be considered in future studies,
 especially in patients with residual findings such as thrombocyto-
 sis or thrombosis.

We also explored dosing regimens because ecizumab is
 extremely expensive, and insurance/health agencies are reluctant
 to pay for off-label use. The previous study recommended an aug-
 mented induction regimen based on the theory that PLE would
 limit drug effectiveness, at least early during treatment^{3,13}. However,
 we found that this was unnecessary. Our measurements of ecizi-
 zumab, total C5 (C5 + ecizumab), AH50 and CH50 showed that
 inhibitory blood concentrations were achieved rapidly, indicating
 that lymphatic leakage and PLE were surprisingly quickly mended.
 We also spaced out dosing intervals and found that almost half of

483 the patients required only 30-day maintenance doses, which sub-
 484 stantially reduced the cost.

485 Serum proteomics revealed that GI disease and protein-wasting
 486 in patients with CHAPLE disease cause a starvation state, thereby
 487 explaining the physiological abnormalities in growth, activity and
 488 maturation. We found that the downregulated proteins were mostly
 489 rescued (23 of 26) by treatment, likely due to the prevention of lymph
 490 protein loss and anabolic processes. In intestinal lymphangiectasia,
 491
 492
 493
 494
 495
 496
 497
 498
 499
 500
 501
 502
 503
 504
 505
 506
 507
 508
 509
 510
 511
 512
 513
 514
 515
 516
 517
 518
 519
 520
 521
 522
 523
 524
 525
 526
 527
 528
 529
 530
 531
 532
 533
 534
 535
 536
 537
 538
 539
 540
 541
 542
 543
 544
 545
 546
 547
 548

albumin and immunoglobulins are specifically lost^{38,39}. We now
 show that immunoregulatory proteins with structural immuno-
 globulin domains are also selectively lost⁴⁰. By contrast, only 18
 of 68 upregulated proteins showed a significant correction with
 treatment. We conjecture that, because eculizumab blocks at the
 level of C5, immune activation and inflammation due to upstream
 C3a anaphylatoxin and C3b opsonization induces these pro-
 teins in a self-perpetuating process despite eculizumab therapy⁴¹.

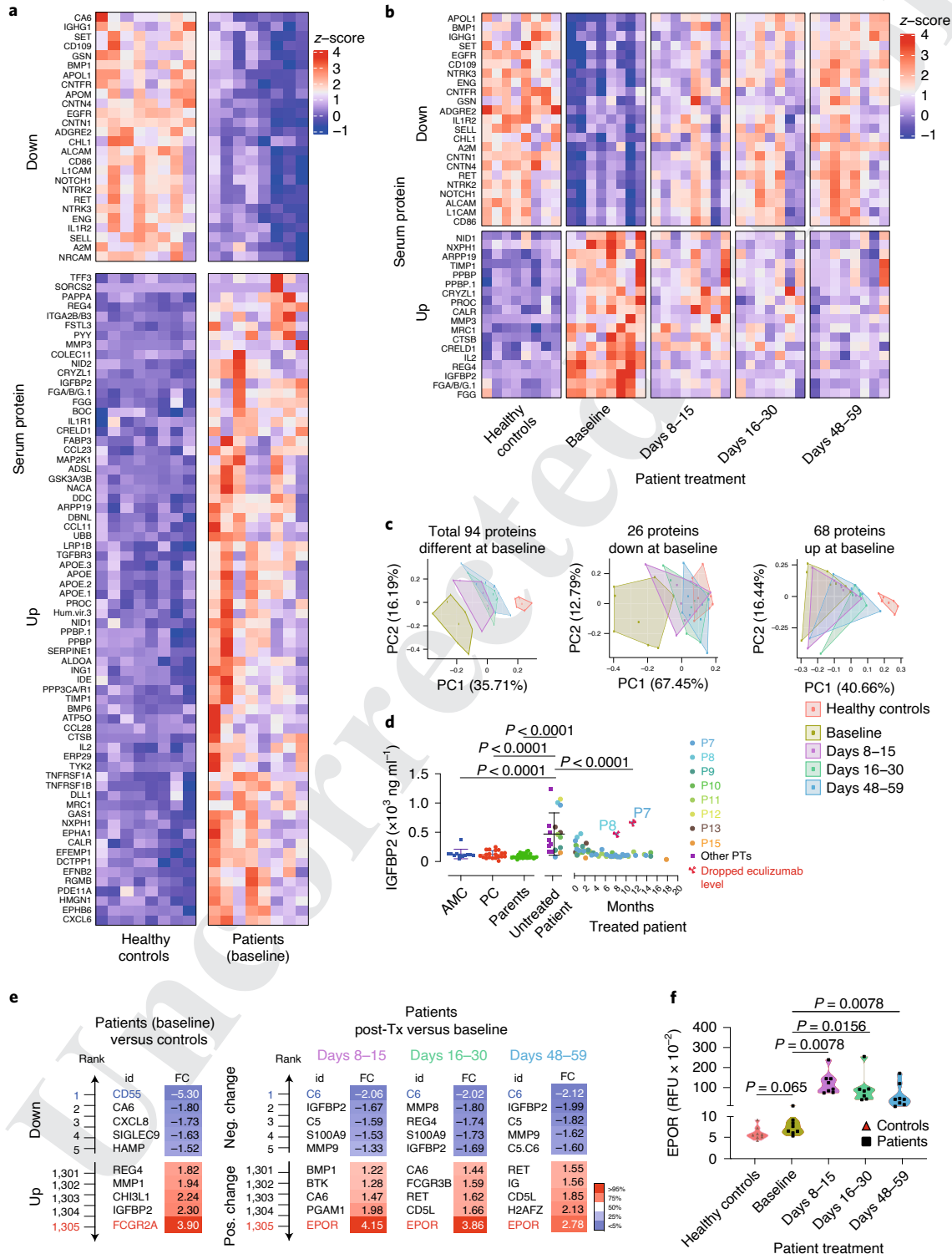


Fig. 6 | Serum proteins altered in patients and response to eculizumab therapy. **a**, Compared with healthy AMC, patients at baseline showed 94 proteins with differences significant at $P < 0.05$ (two-sided) after correcting for multiple testing of all 1305 proteins measured; 26 of these proteins were downregulated and 68 were upregulated in the patients. **b**, Comparing baseline to post-treatment timepoints for the patients up to day 59 showed 41 proteins with differences significant at $P < 0.05$ (two-sided) after correcting for multiple testing of the 94 proteins analyzed due to a difference at baseline. All 41 proteins changed towards the level observed in healthy controls. **c**, PCA plots using all 94 proteins or separately those down- or upregulated in patients at baseline. **d**, Serum IGFBP2 concentrations. Statistics used an ordinary one-way ANOVA with Dunnett's multiple comparisons correction (numbers of samples: 12 AMC, 20 unrelated processing controls (PC), 36 parent samples, 20 samples from 14 untreated patients, 61 samples from 8 patients post-treatment). Error bars indicate mean and s.d. values. **e**, Top and bottom five proteins, ranked according to calculated $\log_2(\text{FC})$ values, where FC means fold change, either in reference to controls (at baseline), or to pretreatment levels in the patients at the indicated timepoints (during eculizumab treatment). **f**, EPOR levels in RFU are shown. Comparison of healthy controls to baseline was made by Mann-Whitney test and inpatient comparisons by Wilcoxon matched-pairs signed-rank test (two-sided P value; $n = 8$ patients, and eight AMC in **a-d** and **f**). The violin plots show the distribution of values across the minimum to maximum range. Protein measurements were performed on the SOMAlogic platform except for IGFBP2 in **d**, which was determined by ELISA. PC1, principal component 1; PC2, principal component 2; Pos., positive; Neg., negative.

549 Interestingly, eculizumab treatment increased C3 and inacti-
550 vated C3b. Similar changes occur in PNH following eculizumab,
551 with erythrocytes accumulating C3d on their surface. Opsonized
552 erythrocytes undergo extravascular hemolysis, reducing the treat-
553 ment benefits⁴². Interestingly, total C4 concentration was elevated
554 in patients with CHAPLE disease with four or six C4 gene cop-
555 ies. We also found that an SNP encoding the V802I amino acid
556 substitution in C5 protein alters the blood concentration of the
557 eculizumab-bound C5 complex, with potential effects on alterna-
558 tive C5 activation through human neutrophil elastase¹⁷. Our data
559 suggests that these genetic factors may modify disease activity and
560 pharmacodynamic properties of eculizumab in CHAPLE disease.

561 Our proteomics revealed multiple coagulation factor abnormali-
562 ties. Thus, CHAPLE disease involves the pathological cross-talk of
563 complement abnormalities on coagulation similar to glycosylation
564 disorders that also present with lymphangiectasia and coagula-
565 tion abnormalities⁴³. Further studies are needed to understand the
566 intersection of complement and coagulation pathways, especially
567 in unexplained lymphangiectasia disorders. Interestingly, we found
568 IGFBP2 to be a sensitive biomarker. High IGFBP2 concentrations
569 were reported in various kidney diseases⁴⁴. It is highly expressed
570 in different cancers and promotes angiogenesis by enhancing vas-
571 cular endothelial growth factor (VEGF) expression⁴⁵. We did not
572 detect an apparent renal phenotype in CHAPLE; perhaps the bio-
573 logical IGFBP2 activity may be relevant to the circulatory features⁴⁶.
574 Unexpectedly, we found eculizumab treatment was also associ-
575 ated with increases in certain serum proteins that were normal in
576 untreated disease. The EPOR showed the largest increase. Recent
577 studies indicate that the EPOR is expressed in endothelial cells and
578 is essential for healthy vasculature and vessel repair^{36,37}. Thus, EPOR
579 function may contribute to the therapeutic effects of eculizumab in
580 healing damaged GI lymphatic vessels.

581 Genetic deficiencies of the complement inhibitors CD46, CD55
582 and CD59 reveal protective roles in different organs. Germline
583 CD55 deficiency in CHAPLE disease, like atypical hemolytic ure-
584 mic syndrome, causes abnormalities in coagulation, hematopoietic
585 cells and endothelium, although it has a selective impact on the GI
586 lymphatic vasculature. CD55 is upregulated by diverse stress or dan-
587 ger signals, suggesting that it has cytoprotective roles during inflam-
588 mation, coagulation and angiogenesis⁴⁷. The same set of stimuli may
589 not produce an identical response in CD46 or CD59, implying that
590 the dominant inhibitor is context-dependent⁴⁸. For example, CD59
591 is expressed by blood vascular endothelial cells but is absent in lym-
592 phatic endothelium⁴⁹. PNH involves a somatic mutation in eryth-
593 rocytes, so presumably CD55 and CD59 are intact in the gut and
594 prevent GI manifestations⁹.

595 Gut microbiota may provide the constant stimulus to comple-
596 ment activation in CHAPLE disease. Our metagenomic profiling
597 showed that patients with CHAPLE disease have pathological
598 microbiota such as inflammation-associated *Enterobacteriaceae* and
599 reduced Shannon diversity. These are signs of a diseased GI tract and

might provide the impetus for ongoing local complement hyperac-
tivation. We found greater interpatient dissimilarity of microbiota
before treatment, and homogenization afterwards. This is consis-
tent with the 'Anna Karenina' principle, whereby GI diseases cause
distinct abnormal microbiota profiles in different patients, whereas
microbiota configurations in healthy people converge toward a
more homogeneous structure⁵⁰. Eculizumab treatment removes
microbiota stressors and rebalances a healthy microbiome.

Online content

Any methods, additional references, Nature Research report-
ing summaries, source data, extended data, supplementary infor-
mation, acknowledgements, peer review information; details of
author contributions and competing interests; and statements of
data and code availability are available at <https://doi.org/10.1038/s41590-020-00830-z>.

Received: 18 June 2020; Accepted: 28 October 2020;

References

1. Waldmann, T. A., Steinfeld, J. L., Dutcher, T. F., Davidson, J. D. & Gordon, R. S. Jr. The role of the gastrointestinal system in 'idiopathic hypoproteinemia'. *Gastroenterology* **41**, 197–207 (1961).
2. Ozen, A. et al. CD55 deficiency, early-onset protein-losing enteropathy, and thrombosis. *N. Engl. J. Med.* **377**, 52–61 (2017).
3. Kurolap, A. et al. Loss of CD55 in eculizumab-responsive protein-losing enteropathy. *N. Engl. J. Med.* **377**, 87–89 (2017).
4. Ozen, A. CHAPLE syndrome uncovers the primary role of complement in a familial form of Waldmann's disease. *Immunol. Rev.* **287**, 20–32 (2019).
5. Mevorach, D. Clearance of dying cells and systemic lupus erythematosus: the role of C1q and the complement system. *Apoptosis* **15**, 1114–1123 (2010).
6. Holers, V. M. Complement and its receptors: new insights into human disease. *Annu. Rev. Immunol.* **32**, 433–459 (2014).
7. Kwan, W. H., van der Touw, W. & Heeger, P. S. Complement regulation of T cell immunity. *Immunol. Res.* **54**, 247–253 (2012).
8. Elvington, M., Liszewski, M. K. & Atkinson, J. P. Evolution of the complement system: from defense of the single cell to guardian of the intravascular space. *Immunol. Rev.* **274**, 9–15 (2016).
9. Zipfel, P. F. & Skerka, C. Complement regulators and inhibitory proteins. *Nat. Rev. Immunol.* **9**, 729–740 (2009).
10. Rother, R. P., Rollins, S. A., Mojciak, C. F., Brodsky, R. A. & Bell, L. Discovery and development of the complement inhibitor eculizumab for the treatment of paroxysmal nocturnal hemoglobinuria. *Nat. Biotechnol.* **25**, 1256–1264 (2007).
11. Wong, E. K., Goodship, T. H. & Kavanagh, D. Complement therapy in atypical haemolytic uraemic syndrome (aHUS). *Mol. Immunol.* **56**, 199–212 (2013).
12. Harris, C. L., Pouw, R. B., Kavanagh, D., Sun, R. & Ricklin, D. Developments in anti-complement therapy; from disease to clinical trial. *Mol. Immunol.* **102**, 89–119 (2018).
13. Kurolap, A. et al. Eculizumab is safe and effective as a long-term treatment for protein-losing enteropathy due to CD55 deficiency. *J. Pediatr. Gastroenterol. Nutr.* **68**, 325–333 (2019).
14. Di Narzo, A. F. et al. High-throughput identification of the plasma proteomic signature of inflammatory bowel disease. *J. Crohns Colitis* **13**, 462–471 (2019).
15. Pickard, J. M., Zeng, M. Y., Caruso, R. & Nunez, G. Gut microbiota: role in pathogen colonization, immune responses, and inflammatory disease. *Immunol. Rev.* **279**, 70–89 (2017).

16. Schwertz, A. et al. Microbiota in pediatric inflammatory bowel disease. *J. Pediatr.* **157**, 240–244.e241 (2010).
17. Giles, J. L., Choy, E., van den Berg, C., Morgan, B. P. & Harris, C. L. Functional analysis of a complement polymorphism (rs17611) associated with rheumatoid arthritis. *J. Immunol.* **194**, 3029–3034 (2015).
18. Hillebrandt, S. et al. Complement factor 5 is a quantitative trait gene that modifies liver fibrogenesis in mice and humans. *Nat. Genet.* **37**, 835–843 (2005).
19. Schatz-Jakobsen, J. A. et al. Structural basis for eculizumab-mediated inhibition of the complement terminal pathway. *J. Immunol.* **197**, 337–344 (2016).
20. Fukuzawa, T. et al. Long lasting neutralization of C5 by SKY59, a novel recycling antibody, is a potential therapy for complement-mediated diseases. *Sci. Rep.* **7**, 1080 (2017).
21. Zelek, W. M., Taylor, P. R. & Morgan, B. P. Development and characterization of novel anti-C5 monoclonal antibodies capable of inhibiting complement in multiple species. *Immunology* **157**, 283–295 (2019).
22. Ardissino, G. et al. Complement functional tests for monitoring eculizumab treatment in patients with atypical hemolytic uremic syndrome: an update. *Pediatr. Nephrol.* **33**, 457–461 (2018).
23. Lintner, K. E. et al. Early components of the complement classical activation pathway in human systemic autoimmune diseases. *Front Immunol.* **7**, 36 (2016).
24. Yang, Y. et al. Gene copy-number variation and associated polymorphisms of complement component C4 in human systemic lupus erythematosus (SLE): low copy number is a risk factor for and high copy number is a protective factor against SLE susceptibility in European Americans. *Am. J. Hum. Genet.* **80**, 1037–1054 (2007).
25. Saxena, K. et al. Great genotypic and phenotypic diversities associated with copy-number variations of complement C4 and RP-C4-CYP21-TNX (RCCX) modules: a comparison of Asian-Indian and European American populations. *Mol. Immunol.* **46**, 1289–1303 (2009).
26. Dahm, A. E. A. et al. Elevated complement C3 and C4 levels are associated with postnatal pregnancy-related venous thrombosis. *Thromb. Haemost.* **119**, 1481–1488 (2019).
27. Savelli, S. L. et al. Opposite profiles of complement in antiphospholipid syndrome (APS) and systemic lupus erythematosus (SLE) among patients with antiphospholipid antibodies (aPL). *Front Immunol.* **10**, 885 (2019).
28. Medof, M. E., Walter, E. I., Rutgers, J. L., Knowles, D. M. & Nussenzweig, V. Identification of the complement decay-accelerating factor (DAF) on epithelium and glandular cells and in body fluids. *J. Exp. Med.* **165**, 848–864 (1987).
29. Kostic, A. D. et al. Genomic analysis identifies association of *Fusobacterium* with colorectal carcinoma. *Genome Res* **22**, 292–298 (2012).
30. Arthur, J. C. et al. Intestinal inflammation targets cancer-inducing activity of the microbiota. *Science* **338**, 120–123 (2012).
31. Lloyd-Price, J. et al. Multi-omics of the gut microbial ecosystem in inflammatory bowel diseases. *Nature* **569**, 655–662 (2019).
32. Vujkovic-Cvijin, I. et al. Dysbiosis of the gut microbiota is associated with HIV disease progression and tryptophan catabolism. *Sci. Transl. Med.* **5**, 193ra191 (2013).
33. Olm, M. R. et al. Necrotizing enterocolitis is preceded by increased gut bacterial replication, *Klebsiella*, and fimbriae-encoding bacteria. *Sci. Adv.* **5**, eaax5727 (2019).
34. Shin, N. R., Whon, T. W. & Bae, J. W. Proteobacteria: microbial signature of dysbiosis in gut microbiota. *Trends Biotechnol.* **33**, 496–503 (2015).
35. Blanton, L. V. et al. Gut bacteria that prevent growth impairments transmitted by microbiota from malnourished children. *Science* **351**, aad3311–aad3311 (2016).
36. Heeschen, C. et al. Erythropoietin is a potent physiologic stimulus for endothelial progenitor cell mobilization. *Blood* **102**, 1340–1346 (2003).
37. Ribatti, D. et al. Human erythropoietin induces a pro-angiogenic phenotype in cultured endothelial cells and stimulates neovascularization in vivo. *Blood* **93**, 2627–2636 (1999).
38. Homburger, F. & Petermann, M. L. Studies on hypoproteinemia; familial idiopathic dysproteinemia. *Blood* **4**, 1085–1108 (1949).
39. Parfitt, A. M. Familial neonatal hypoproteinaemia with exudative enteropathy and intestinal lymphangiectasis. *Arch. Dis. Child* **41**, 54–62 (1966).
40. Srinivasan, M. & Roeske, R. W. Immunomodulatory peptides from IgSF proteins: a review. *Curr. Protein Pept. Sci.* **6**, 185–196 (2005).
41. Sauter, R. J. et al. Functional relevance of the anaphylatoxin receptor C3aR for platelet function and arterial thrombus formation marks an intersection point between innate immunity and thrombosis. *Circulation* **138**, 1720–1735 (2018).
42. Notaro, R. & Sica, M. C3-mediated extravascular hemolysis in PNH on eculizumab: mechanism and clinical implications. *Semin Hematol.* **55**, 130–135 (2018).
43. Brucker, W. J. et al. An emerging role for endothelial barrier support therapy for congenital disorders of glycosylation. *J. Inher. Metab. Dis.* **43**, 880–890 (2020).
44. Ding, H., Kharboutli, M., Saxena, R. & Wu, T. Insulin-like growth factor binding protein-2 as a novel biomarker for disease activity and renal pathology changes in lupus nephritis. *Clin. Exp. Immunol.* **184**, 11–18 (2016).
45. Azar, W. J. et al. IGFBP-2 enhances VEGF gene promoter activity and consequent promotion of angiogenesis by neuroblastoma cells. *Endocrinology* **152**, 3332–3342 (2011).
46. Ozen, A., Comrie, W. A. & Lenardo, M. J. CD55 deficiency and protein-losing enteropathy. *N. Engl. J. Med.* **377**, 1499–1500 (2017).
47. Mason, J. C., Lidington, E. A., Ahmad, S. R. & Haskard, D. O. bFGF and VEGF synergistically enhance endothelial cytoprotection via decay-accelerating factor induction. *Am. J. Physiol. Cell Physiol.* **282**, C578–C587 (2002).
48. Mason, J. C. et al. Induction of decay-accelerating factor by cytokines or the membrane-attack complex protects vascular endothelial cells against complement deposition. *Blood* **94**, 1673–1682 (1999).
49. Park, S. M. et al. Mapping the distinctive populations of lymphatic endothelial cells in different zones of human lymph nodes. *PLoS One* **9**, e94781 (2014).
50. Zaneveld, J. R., McMinds, R. & Vega Thurber, R. Stress and stability: applying the Anna Karenina principle to animal microbiomes. *Nat. Microbiol.* **2**, 17121 (2017).

Publisher's note Springer Nature remains neutral with regard to jurisdictional claims in published maps and institutional affiliations.

© The Author(s), under exclusive licence to Springer Nature America, Inc. 2020